Behavior study of the generalized-strain mesh-free method (GSMF)

†Wilber Vélez[1], Tiago Oliveira[2], and Artur Portela[1]

[1,] Department of Civil and Environmental Engineering, University of Brasília, BR.

*Presenting author: wilbervelez@hotmail.com
†Corresponding author: aportela@unb.br

Abstract

The generalized-strain mesh-free (GSMF) local method, it is derived through a weighted-residual formulation that leads to the work theorem of structures theory. In a local region, the work theorem establishes an energy relationship between a statically – admissible stress field and an independent kinematically – admissible strain field.

In the formulation of the GSMF, the local form of work theorem is simply an integration – free formula. The Moving Least Squares (MLS) approximation of the elastic field is used to construct the trial function in this local meshless formulation. GSMF has a highly computational efficiency leading to accurate numerical results in two-dimensional elasticity problems.

This paper is concerned with the size effect of the configuration parameters of the local support domain and the local weighted-residual or quadrature/collocation domain on GSMF. A comparison of the error in energy and displacement is presented for five different regular nodal distribution, in order to solve the Timoshenko cantilever beam problem and the infinite plate with circular hole. The results are compared with the exact solution and optimal parameters have been determined.

Keywords: Generalized-Strain Mesh-Free (GSMF), work theorem, Moving Least Squares (MLS), local support domain, local weighted-residual domain.

Introduction

There are different numerical modeling techniques and the most popular and widely used is the Finite Element Method (FEM). Although recently meshless methods are becoming more used due to their accuracy and performance in numerical analysis. Different methods have been proposed [1-7], some of them are derived from a weak – form formulation on global domain and others from local sub – domains. The weighted – residual method is the basis for the meshless formulation [8].

The Generalized – Strain Mesh – free (GSMF) formulation presented by [9], expressed that the work theorem generates a weak form that is completely integration free, working as a weighted-residual weak – form collocation. This formulation has two important parameters associated to support and quadrature/collocation domain, this parameters have a greater influence in the problem solution obtained by Meshfree methods.

The size local support domain (α_s) and the weak – form domain or local quadrature/collocation domain (α_q) are very important meshless parameter, both related to accuracy and computational efficiency. A comparative study of the effect of these size parameters using the Meshless Local Petrov – Galerkin method (MLPG) for the solution of a cantilever beam was presented by [10] and, using the same method, a similar study for the cantilever beam and the infinite plate with circular hole was carried out by [11].

This paper presents a numerical comparison of the Generalized-strain Mesh-free (GSMF) formulation for the size effect of the configuration parameters of the local support domain and the local quadrature/collocation domain; for five different regular nodal distribution of the Timoshenko cantilever beam and one nodal distribution of the infinite plate with circular hole. The results obtained in this work, both for the energy and displacement, are compared with the exact solution presented for 2D problems plane stress case and important conclusions are presented in the end.

MLS Approximation

Let Ω be the domain of a body with boundary Γ and let $N = \{X_1, X_2, .., X_N\} \in \Omega$ be a set of scattered nodal points that represents a meshless discretization. Some of them are located on the boundary Γ where Ω_s, represented as Ω_P, Ω_Q and Ω_R, is the local compact support of a node X_t, represented as X_P, X_Q and X_R. Ω_x is the domain of definition of a sampling point X and Ω_q is the local weak-form domain or quadrature domain of node X_i, as represent in Fig. 1.

Circular or rectangular local supports centered at each nodal point can be used. In the region of a sampling point X, the domain of definition of MLS approximation is the subdomain Ω_x, where the approximation is defined.

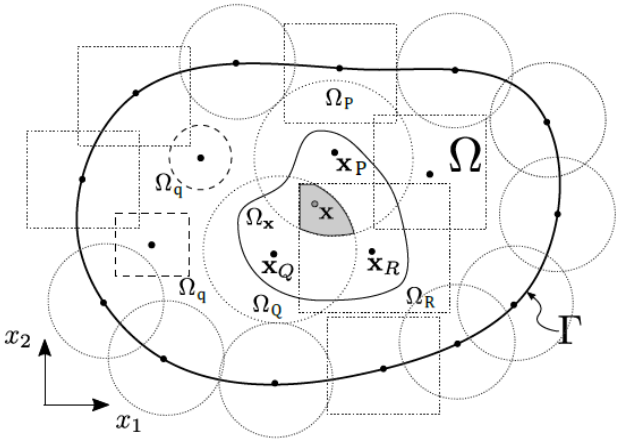

Figure 1. Representation of a global domain Ω and boundary Γ in a meshless discretization, with Xi nodes distributed within the body.

Shape Functions

Let Ω_x be the domain of definition of the MLS approximation, in a neighborhood of a sampling point x. To approximate the displacement $u(x) \in \Omega_x$, over a number of scattered nodes $X_i \in \Omega$, $i = 1, 2, .., n$, where the nodal parameters $\hat{u}_i$ are defined, the MLS approximation is given by

$$u^h(x) = \mathbf{p}^T(x)a(x), \tag{1}$$

for $x \in \Omega_x$, in which

$$\mathbf{p}^T(x) = \left[p_1(x), p_2(x), ..., p_m(x)\right], \tag{2}$$

is a vector of the complete monomial basis of order m and a(x) is the vector of unknown coefficients $a_j(x)$, $j = 1, 2, ..., m$ that are functions of the space coordinates $x = \left[x_1, x_2\right]^T$, for 2-D problems.

The coefficient vector a(x) is determined by minimizing the weighted discrete L_2 norm

$$J(x)=\frac{1}{2}\sum_{i=1}^{n}w_i(x)\left[u^h(x_i)-\hat{u}_i\right]^2=\frac{1}{2}\sum_{i=1}^{n}w_i(x)\left[\mathbf{p}^T(x_i)a(x)-\hat{u}_i\right]^2, \tag{3}$$

with respect to each term of a(x), in which $w_i(x)$ is the weight function associated with the node x_i, with the compact support that is $w_i(x)>0$, for all x in the support of $w_i(x)$. In the Fig. 1 is represented the compact support of the MLS weight functions associated with a few nodes. Finding the extremum of *J(x)* with respect to each term of a(x), leads to

$$\mathbf{A}(x)\mathrm{a}(x)=\mathbf{B}(x)\hat{\mathbf{u}}, \tag{4}$$

where,

$$\mathbf{A}(x)=\sum_{i=1}^{n}w_i(x)\mathbf{p}(x_i)\mathbf{p}^T(x_i), \tag{5}$$

$$\mathbf{B}(x)=\left[w_1(x)\mathbf{p}(x_1),w_2(x)\mathbf{p}(x_2),...,w_n(x)\mathbf{p}(x_n)\right] \tag{6}$$

and

$$\hat{\mathbf{u}}=\left[\hat{u}_1,\hat{u}_2,...,\hat{u}_n\right]. \tag{7}$$

Solving equation (4) for a(x) yields

$$\mathrm{a}(x)=\mathbf{A}^{-1}(x)\mathbf{B}(x)\hat{\mathbf{u}}, \tag{8}$$

Provided $n \geq m$, for each some point x, condition defined in the MLS approximation.

$$u^h(x)=\sum_{i=1}^{n}\phi_i(x)\hat{u}_i, \tag{9}$$

in which

$$\phi_i(x)=\sum_{i=1}^{n}p_j(x)\left[\mathbf{A}^{-1}(x)\mathbf{B}(x)\right]_{ji} \tag{10}$$

The shape function of the MLS approximation for the node x_i is represented Figure 2.

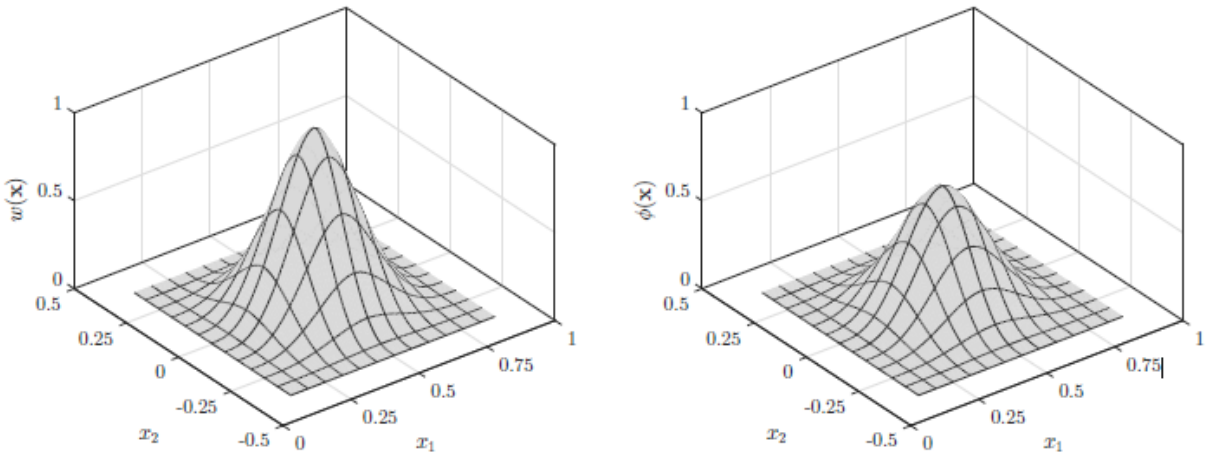

Figure 2. Respectively the typical weight function and shape function of the MLS approximation

The MLS shape functions are not nodal interpolants which means mathematically that Since $\phi_i(x_j)\neq\delta_{ij}$. Since $\phi_i(x)$ vanishes for *x* not in the local domain of the node x_i, is preserved the local

character of the MLS approximation. The nodal shape function is complete up to the order of the basis. The smoothness of the nodal shape function is determined by the smoothness of the basis and of the weight function. The spatial derivatives of the shape function $\phi_i(x)$ are giving by

$$\phi_{i,k}(x) = \sum_{j=1}^{m} \left[p_{j,k} \left(\mathbf{A}^{-1}\mathbf{B} \right)_{ji} + p_j \left(\mathbf{A}^{-1}\mathbf{B}_{,k} - \mathbf{A}^{-1}\mathbf{A},_k \, \mathbf{A}^{-1}B \right)_{ji} \right], \tag{11}$$

in which $()_{,k} = \partial() / \partial x_k$.

Weight Functions

In the Figure 2 the weight functions are represented, in Eq. (3) are introduced for each node x_i, have a compact support for all x, which defines the subdomain where $w_i(x) > 0$. This paper considers rectangular compact supports with weight functions defined as

$$w_i(x) = w_{i_x}(x) w_{i_y}(x) \tag{12}$$

the weight function is given by the quartic spline function

$$w_{i_x}(x) = \begin{cases} 1 - 6\left(\frac{d_{i_x}}{r_{i_x}}\right)^2 + 8\left(\frac{d_{i_x}}{r_{i_x}}\right)^3 - 3\left(\frac{d_{i_x}}{r_{i_x}}\right)^4 & for \;\; 0 \le d_{i_x} \le r_{i_x} \\ 0 & for \;\; d_{i_x} > r_{i_x} \end{cases} \tag{13}$$

And

$$w_{i_y}(x) = \begin{cases} 1 - 6\left(\frac{d_{i_y}}{r_{i_y}}\right)^2 + 8\left(\frac{d_{i_y}}{r_{i_y}}\right)^3 - 3\left(\frac{d_{i_y}}{r_{i_y}}\right)^4 & for \;\; 0 \le d_{i_y} \le r_{i_y} \\ 0 & for \;\; d_{i_y} > r_{i_y} \end{cases} \tag{14}$$

in which $d_{i_x} = \|x - x_i\|$ and $d_{i_y} = \|y - y_i\|$. The parameters r_{i_x} and r_{i_y} represent the size of the support for the node i, respectively in the x and y directions.

Elastic Field

The elastic field is approximated at a sampling point x. Considering Eq. (9) the displacement and strain components

$$\mathbf{u} = \begin{bmatrix} u^h(x) \\ v^h(x) \end{bmatrix} = \begin{bmatrix} \phi_1(x) & 0 & \dots & \phi_n(x) & 0 \\ 0 & \phi_1(x) & \dots & 0 & \phi_n(x) \end{bmatrix} \begin{bmatrix} \hat{u}_1 \\ \hat{v}_1 \\ \vdots \\ \hat{u}_n \\ \hat{v}_n \end{bmatrix} = \mathbf{\Phi}\hat{\mathbf{u}} \tag{15}$$

$$\varepsilon = \mathbf{L}\mathbf{u} = \mathbf{L}\mathbf{\Phi}\hat{\mathbf{u}} = \mathbf{B}\hat{\mathbf{u}} \tag{16}$$

in which geometrical linearity is assumed in the differential operator **L** and thus,

$$\mathbf{B} = \begin{bmatrix} \phi_{1,1} & 0 & \dots & \phi_{n,1} & 0 \\ 0 & \phi_{1,2} & \dots & 0 & \phi_{n,2} \\ \phi_{2,1} & \phi_{1,1} & \dots & \phi_{n,2} & \phi_{n,1} \end{bmatrix} \tag{17}$$

Stress and traction components are

$$\boldsymbol{\sigma} = \mathbf{D}\varepsilon = \mathbf{DB}\hat{\mathbf{u}} \tag{18}$$

and

$$\mathbf{t} = \mathbf{n}\boldsymbol{\sigma} = \mathbf{nDB}\hat{\mathbf{u}} \tag{19}$$

in which **D** is the matrix of the elastic constants and **n** is the matrix of the components of the unit outward normal, defined as

$$\mathbf{n} = \begin{bmatrix} n_1 & 0 & n_2 \\ 0 & n_2 & n_1 \end{bmatrix} \tag{20}$$

Eq. (15) to (19) show that the variables of the elastic field are defined in terms of the nodal unknowns $\hat{u}$, for all point x ϵ Ω_x.

Local Form of the Work Theorem

The development for the local form of the work theorem introduced in [12] is presented in this section. Let Ω be the domain of a body and Γ its boundary, subdivided in Γ_u and Γ_t that is $\Gamma = \Gamma_u \cup \Gamma_t$; in the Fig. 3 show the nodal points *P, Q* and *R* have corresponding local domains Ω_P, Ω_Q, and Ω_R.

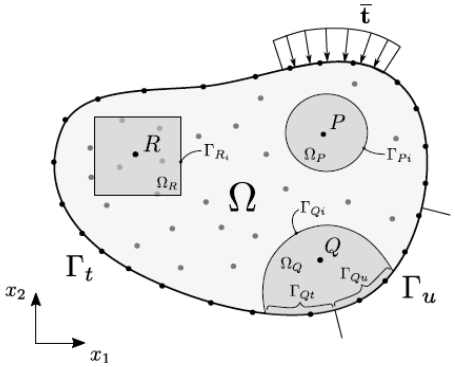

Figure 3. Meshless discretization of the global domain Ω and the local domains Ω_P, Ω_Q and Ω_R, with boundary $\Gamma = \Gamma_u \cup \Gamma_t$ represented.

The mixed fundamental boundary value problem of linear electrostatics aims to determine the distribution of stress σ, strains ε and displacements u throughout the body, when it has constrained displacements $\bar{u}$ defined on Γ_u and is loaded by an external system of distributed surface and body forces with densities denoted by $\bar{\mathbf{t}}$ on Γ_t and b in Ω, respectively.

The entire admissible elastic field is the solution of the posed problem that simultaneously satisfies the kinematic admissibility and the static admissibility. If this solution exists, it can be shown that it is unique, provided linearity and stability of the material are admitted [12, 13].

The general work theorem establishes an energy relationship between any statically – admissible stress field and any kinematically – admissible strain field that can be defined in the body. Derived as a weighted residual statement, the work theorem serves as a unifying basis for the formulation of numerical models Continuum Mechanics [14].

In the domain of the body, consider a statically-admissible stress field that is

$$\mathbf{L}^T\sigma + b = 0 \tag{21}$$

in the domain Ω, with boundary conditions

$$t = n\sigma = \bar{t} \tag{22}$$

on the static boundary Γ_t, σ: Stress components, L: Matrix differential operator, t: represent the traction components, $\bar{\mathbf{t}}$: Prescribed tractions values, n: Unit normal components to the boundary.

In the global domain Ω, consider an arbitrary local subdomain Ω_Q, centered at the point Q, with boundary $\Gamma = \Gamma_{Qi} \cup \Gamma_{Qt} \cup \Gamma_{Qu}$, Γ_{Qi}: Interior local boundary and Γ_{Qt} and Γ_{Qu}: Local boundaries that respectively share a global boundary. Due to its arbitrariness, this local domain can be overlapping with other similar subdomains. For the local domain Ω_Q the strong form of the weighted-residual equation is written as

$$\int_{\Omega_Q} \left(\mathbf{L}^T\sigma + b\right)^T \mathbf{W}_\Omega d\Omega + \int_{\Gamma_{Qt}} (t - \bar{t})^T \mathbf{W}_\Gamma d\Gamma = 0 \tag{23}$$

in which W_Ω and W_Γ are arbitrary weighting functions defined, respectively in Ω and on Γ. When the domain term of Eq. (23) is integrated by parts, the following local weak form of the weighted residual equation is obtained

$$\int_{\Gamma_Q} (\mathbf{n}\boldsymbol{\sigma})^T \mathbf{W}_\Omega d\Gamma - \int_{\Omega_Q} (\boldsymbol{\sigma}^T \mathbf{L}\mathbf{W}_\Omega - \mathbf{b}^T \mathbf{W}_\Omega) d\Omega + \int_{\Gamma_{Qt}} (\mathbf{t} - \bar{\mathbf{t}})^T \mathbf{W}_\Gamma d\Gamma = 0 \tag{24}$$

which now requires continuity of $\mathbf{W}_\Omega$, as an admissibility condition for integrability. For the sake of convenience, the arbitrary weighting function $\mathbf{W}_\Gamma$ is chosen as

$$\mathbf{W}_\Gamma = -\mathbf{W}_\Omega \tag{25}$$

on the boundary Γ_{Qt}. Thus, Eq. (24) leads to

$$\int_{\Gamma_Q} (\mathbf{n}\boldsymbol{\sigma})^T \mathbf{W}_\Omega d\Gamma - \int_{\Omega_Q} (\boldsymbol{\sigma}^T \mathbf{L}\mathbf{W}_\Omega - \mathbf{b}^T \mathbf{W}_\Omega) d\Omega + \int_{\Gamma_{Qt}} (\mathbf{t} - \bar{\mathbf{t}})^T \mathbf{W}_\Gamma d\Gamma = 0 \tag{26}$$

Consider further an arbitrary kinematically-admissible strain field ε^*, with continuous displacements u* and small derivatives, in order to assume geometrical linearity, defined in the global domain that is

$$\varepsilon^* = \mathbf{L}\mathbf{u}^* \tag{27}$$

in the domain Ω, with boundary conditions

$$\mathbf{u}^* = \bar{\mathbf{u}} \tag{28}$$

on the kinematic boundary Γ_u.

When the continuous arbitrary weighting function $\mathbf{W}_\Omega$, is defined as

$$\mathbf{W}_\Omega = \mathbf{u}^* \tag{29}$$

the weak form (26), of the weighted residual equation, becomes

$$\int_{\Gamma_Q-\Gamma_{Qt}-\Gamma_{Qu}} \mathbf{t}^T\mathbf{u}^* d\Gamma + \int_{\Gamma_{Qu}} \mathbf{t}^T\bar{\mathbf{u}}^* d\Gamma + \int_{\Gamma_{Qt}} \bar{\mathbf{t}}^T\mathbf{u}^* d\Gamma - \int_{\Omega_Q} \left(\boldsymbol{\sigma}^T\mathbf{L}\mathbf{u}^* - \mathbf{b}^T\mathbf{u}^*\right) d\Omega = 0 \tag{30}$$

which can be written in a compact form as

$$\int_{\Gamma_Q} \mathbf{t}^T\mathbf{u}^* d\Gamma + \int_{\Omega_Q} \mathbf{b}^T\mathbf{u}^* d\Omega = \int_{\Omega_Q} \boldsymbol{\sigma}^T\varepsilon^* d\Omega \tag{31}$$

This equation is the starting point of kinematically admissible formulations of the local mesh-free method presented in this paper. Equation (31) which expresses the static-kinematic duality, is the local form of the well-known work theorem, the fundamental identity of solid mechanics [16].

It is the important to notice that the stress field $\boldsymbol{\sigma}$, is any one that satisfies equilibrium with the applied external forces **b** and **t**, which is not necessarily the stress field that actually settles in the body. Also, the strain field ε^*, is any one that is compatible with the constrains $\mathbf{u}^* = \bar{\mathbf{u}}$, which is not necessarily the strain field that actually settles in the body. These two fields are not connected function $\mathbf{W}_\Omega$ they are completely independent. For that reason, Eq. (31) can be used under the only assumption of geometrical linearity. It is the independence of the two admissible fields of the Eq. (31) that allows generation of different meshfree methods, when the strain field is locally defined through different options, as carried out in this paper.

A final important remark, worth of mentioning, is that the local domain Ω_Q, is any arbitrary subdomain Ω, of the body.

Modeling Strategy

In the local meshfree methods different formulations can be derived when the arbitrary kinematically – admissible field ε^*, is locally defined in the work theorem, Eq. (31). In the following section, simple kinematically – admissible local fields will be used to derive the meshless formulation presented in this paper, the Generalized-Strain Mesh-Free (GSMF) formulation. On the other hand, the statically – admissible local field $\boldsymbol{\sigma}$, will be always assumed as the elastic field that actually settles in the body. Not only satisfying static admissibility, through Eq. (21) and (22), but also satisfying kinematic admissibility in the elastic field defined as

$$\varepsilon = \mathbf{L}\mathbf{u} \tag{32}$$

In the domain Ω, with boundary conditions

$$\mathbf{u} = \bar{\mathbf{u}} \tag{33}$$

on the kinematic boundary Γu; in the which the displacements u, are assumed continuous with small derivatives, in order to allow for geometrical linearity of the strain field ε. Therefore, Eq. (33) must be enforced in the numerical model, in order to provide a unique solution of the posed problem.

For a meshless discretization of the body, the local weak-form domain or quadrature domain Ω_Q, centered at the node *Q*, can be defined in this paper as a rectangular or circular subdomain, as represented in Fig. 3.

Generalized-Strain Formulation

The Equation (31), the kinematically – admissible displacement field u*, was assumed as a continuous function leading to a regular integral function that is the kinematically-admissible strain field ε^*. For more information about the method, see [9].

However, this continuity assumption on u*, enforced in the local form of the work theorem, is not required but can be relaxed by convenience, provided ε^* can be useful as a generalized function, in the sense of the theory of distributions [15]. Hence, this formulation considers that the kinematically-admissible displacement field is a piece-wise continuous function, defined in terms of the Heaviside step function and therefore the corresponding kinematically-admissible strain field is a generalized function, defined in terms of Dirac delta function.

For the sake of the simplicity, in dealing with Heaviside and Dirac delta functions in a two-dimensional coordinate space, consider a scalar function d, defined as

$$d = \left\| \mathrm{x} - \mathrm{x}_Q \right\| \quad \text{that is} \quad \begin{cases} d = 0 & \text{if} \quad \mathrm{x} \equiv \mathrm{x}_Q \\ d > 0 & \text{if} \quad \mathrm{x} \neq \mathrm{x}_Q \end{cases} \tag{34}$$

which represents the absolute-value function of the distance between a field point x and a particular reference point x_Q, in the local domain $\Omega_Q \bigcup \Gamma_Q$ assigned to the field node Q. Therefore, this definition always assumes $d = d(\mathrm{x},\mathrm{x}_\mathrm{Q}) \geq 0$, as a positive or null vale, in this case when-ever x and x_Q are coincident points. It is important to remark that, in Eq. (34), neither the field point x nor the reference point x_Q is necessarily a nodal point of the local domain.

For a scalar coordinate, $d \supset d(\mathrm{x},\mathrm{x}_\mathrm{Q})$, the Heavise step function can be defined as

$$H(d) = \begin{cases} 1 \text{ if } d \leq 0 \quad (d = 0 \text{ for } \mathrm{x} \equiv \mathrm{x}_\mathrm{Q}) \\ 0 \text{ if } d > 0 \qquad \text{that is } \mathrm{x} \neq \mathrm{x}_\mathrm{Q} \end{cases} \tag{35}$$

in which the discontinuity is assumed at x_Q and consequently, the Dirac delta function is defined with the following properties

$$\delta(d) = H'(d) = \begin{cases} \infty \text{ if } d = 0 \qquad \text{that is } \mathrm{x} \equiv \mathrm{x}_\mathrm{Q} \\ 0 \text{ if } d \neq 0 \quad (d > 0 \text{ for } \mathrm{x} \neq \mathrm{x}_\mathrm{Q}) \end{cases} \quad \text{and} \quad \int_{-\infty}^{+\infty} \delta(d)\mathrm{d}d = 1 \tag{36}$$

in which H'(d) represents the distributional derivate of H(d). Note that the derivate of H(d), with respect to the coordinate x_i, can be defined as

$$H(d)_{,i} = H'(d)d_{,i} = \delta(d)d_{,i} = \delta(d)n_i \tag{37}$$

Since the result of this equation is not affected by any particular value of the constant n_i, this constant will be conveniently redefined later on.

Kronecker delta function can be defined through Heaviside step function as

$$\Delta(d) = H(d) + H(-d) - 1 = \begin{cases} 1 \text{ if } d = 0 \quad \text{that is } \mathrm{x} \equiv \mathrm{x}_\mathrm{Q} \\ 0 \text{ if } d > 0 \quad \text{that is } \mathrm{x} \neq \mathrm{x}_\mathrm{Q} \end{cases} \tag{38}$$

Which has the distributional derivative always null that is

$$\Delta'(d) = \delta(d) - \delta(-d) = \delta(d) - \delta(d) = 0 \tag{39}$$

as a consequence of the symmetry of Dirac delta function.

Now considerer that d_l, d_j and d_k represent the distance function d, defined in Eq. (34), for corresponding field points x_l, x_j and x_k. Then, the kinematically – admissible displacement field can be defined as a linear combination of Kronecker delta function evaluations at an arbitrary number of collocation points, conveniently arranged in the local domain $\Omega_Q \bigcup \Gamma_Q$ of the field node Q, that is

$$\mathrm{u}^*(\mathrm{x}) = \left[\frac{L_i}{n_i} \sum_{l=1}^{n_i} \Delta(d_l) + \frac{L_t}{n_t} \sum_{j=1}^{n_t} \Delta(d_j) + \sum_{k=1}^{n_\Omega} \Delta(d_k) \right] e \tag{40}$$

in which $\mathrm{e} = \begin{bmatrix} 1 & 1 \end{bmatrix}^T$ represents the metric of the orthogonal directions; n_i, n_t and n_Ω represent the number of collocation points, respectively on the local interior boundary $\Gamma_{Q_i} = \Gamma_Q - \Gamma_{Q_t} - \Gamma_{Q_u}$ with length L_i, on the local static boundary Γ_{Q_t} with length L_t and in the local domain Ω_Q with area S. This assumed displacement field u*(x), a discrete rigid-body unit displacement defined at collocation points, schematically represent in Fig. 4, conveniently leads to a null

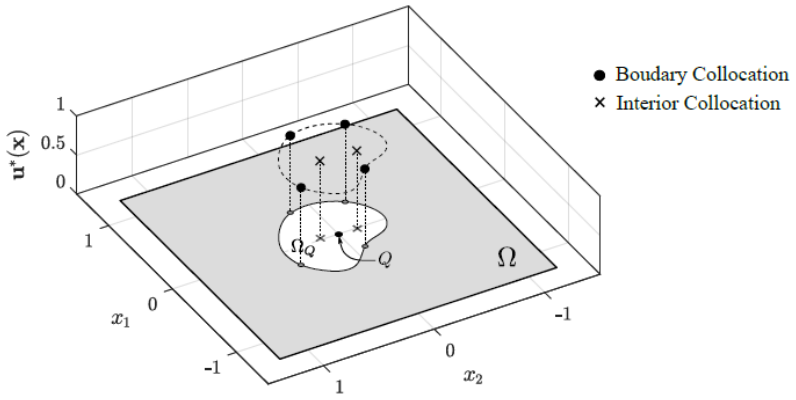

Figure 4. Schematic representation of the displacement u*(x) **of Eq. (38), a discrete rigid-body unit displacement defined at collocation points, of the Generalized-Strain Mesh-free formulation, for a local domain associated with a field node** *Q*.

generalized strain field that is

$$\varepsilon^*(\mathrm{x}) = 0 \tag{41}$$

as a consequence of Eq. (39). The local work theorem, Eq. (31), can be written as

$$\int_{\Gamma_Q - \Gamma_{Qt}} \mathbf{t}^T \mathbf{u}^* d\Gamma + \int_{\Gamma_{Qt}} \overline{\mathbf{t}}^T \mathbf{u}^* d\Gamma + \int_{\Omega_Q} \mathbf{b}^T \mathbf{u}^* d\Omega = \int_{\Omega_Q} \boldsymbol{\sigma}^T \varepsilon^* d\Omega \tag{42}$$

which, after considering the assumed displacement and the strain components of the kinematically-admissible field, respectively Eq. (40) and (41), leads to

$$\frac{L_i}{n_i}\sum_{l=1}^{n_i}\int_{\Gamma_Q-\Gamma_{Qt}}\mathbf{t}^T\Delta(d_l)\mathrm{e}\mathrm{d}\Gamma+\frac{L_t}{n_t}\sum_{j=1}^{n_t}\int_{\Gamma_{Qt}}\bar{\mathbf{t}}^T\Delta(d_j)\mathrm{e}\mathrm{d}\Gamma+\frac{S}{n_\Omega}\sum_{k=1}^{n_\Omega}\int_{\Omega_Q}\mathbf{b}^T\Delta(d_k)\mathrm{d}\Omega=0 \tag{43}$$

Now considering the properties of Kronecker delta function, defined in Eq. (38), the Eq. (43) simply leads to

$$\mathrm{e}^T\left[\frac{L_i}{n_i}\sum_{l=1}^{n_i}t_{\mathrm{x}_l}+\frac{L_t}{n_t}\sum_{j=1}^{n_t}\bar{\mathbf{t}}_{\mathrm{x}_j}+\frac{S}{n_\Omega}\sum_{k=1}^{n_\Omega}\mathbf{b}_{\mathrm{x}_k}\right]=0 \tag{44}$$

and finally to

$$\frac{L_i}{n_i}\sum_{l=1}^{n_i}t_{\mathrm{x}_l}=-\frac{L_t}{n_t}\sum_{j=1}^{n_t}\bar{\mathbf{t}}_{\mathrm{x}_j}-\frac{S}{n_\Omega}\sum_{k=1}^{n_\Omega}\mathbf{b}_{\mathrm{x}_k} \tag{45}$$

Equation (45) states the equilibrium of tractions and body forces, pointwisely defined at collocation points, as schematically represented in Fig. 5; obviously, the pointwise version of the Euler – Cauchy stress principle.

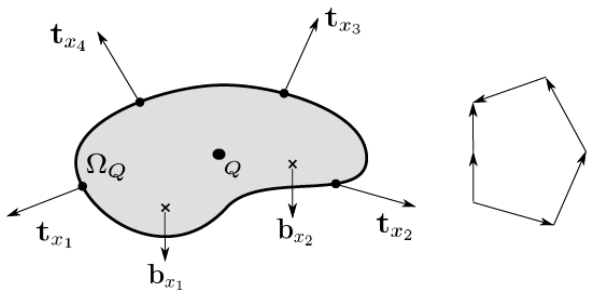

Figure 5. Schematic representation of the equilibrium of tractions and body forces of Eq. (44), pointwisely defined at collocation points of a local domain associated with a field node *Q*, of the Generalized-Strain Mesh-free formulation.

This is the equation used in the GSMF formulation which, therefore, is free of integration. Since the work theorem is a weighted – residual weak form, it can be easily seen that this integration – free formulation is nothing else other than a weighted – residual weak – form collocation.

Equations (45), of the Generalized – Strain Mesh – free formulation, can be derived from another kinematically – admissible displacement field, directly defined in terms of Heaviside step function, see [8].

Discretization of Eq. (45) is carried out with the MLS approximation, Eq. (15) to (19), for the local domain Ω_Q, in terms of the nodal unknowns $\hat{\mathbf{u}}$, thus leading to the system of two linear algebraic equations

$$\frac{L_i}{n_i}\sum_{l=1}^{n_i}\mathbf{n}_{\mathrm{x}_l}\mathbf{D}\mathbf{B}_{\mathrm{x}_l}\hat{\mathbf{u}}=-\frac{L_t}{n_t}\sum_{j=1}^{n_t}\bar{\mathbf{t}}_{\mathrm{x}_j}-\frac{S}{n_\Omega}\sum_{k=1}^{n_\Omega}\mathbf{b}_{\mathrm{x}_k} \tag{46}$$

that can be written as

$$\mathbf{K}_Q\hat{\mathbf{u}}=\mathbf{F}_Q \tag{47}$$

in which K_Q, the nodal stiffness matrix associated with the local Ω_Q, is a *2x2n* matrix given by

$$\mathbf{K}_Q=\frac{L_i}{n_i}\sum_{l=1}^{n_i}\mathbf{n}_{\mathrm{x}_l}\mathbf{D}\mathbf{B}_{\mathrm{x}_l} \tag{48}$$

and F_Q is the respective force vector given by

$$\mathbf{F}_Q = -\frac{L_t}{n_t}\sum_{j=1}^{n_t}\bar{\mathbf{t}}_{x_j} - \frac{S}{n_\Omega}\sum_{k=1}^{n_\Omega}\mathbf{b}_{x_k} \tag{49}$$

Consider that the problem has a total of *N* field nodes *Q,* each one associated with the respective local region Ω_Q. Assembling Eq. (47), for all *M* interior and static – boundary field nodes leads to the global system of *2M x 2N* equations

$$\mathbf{K}\hat{\mathbf{u}} = \mathbf{F} \tag{50}$$

Finally, the remaining equations are obtained from the *N – M* boundary field nodes on the kinematic boundary. For a field node on the kinematic boundary, a direct interpolation method is used to impose the Kinematic boundary condition as

$$u_k^h(\mathrm{x_j}) = \sum_{i=1}^{n}\phi_i(\mathrm{x_j})\hat{u}_{ik} = \bar{\mathbf{u}}_k \tag{51}$$

Or, in matrix form as

$$\mathbf{u}_k = \Phi_k\hat{\mathrm{u}} = \bar{\mathbf{u}}_k \tag{52}$$

with k = 1, 2, where $\bar{\mathbf{u}}_k$ is specified nodal displacement component. Equations (51) are directly assembled into the global system of equations (50).

Numerical Examples

This section presents some numerical results for Cantilever beam and the Plate with a circular hole for different nodal configurations. The effects of the size of local support and quadrature/collocation domain are analyzed and compared with the exact solution.

For a generic node i, the size of the local support ΩS and the local domain of integration Ωq are respectively given by

$$r\Omega_S = \alpha_S c_i, \tag{53}$$

$$r\Omega_q = \alpha_q c_i, \tag{54}$$

in which Ci represents the distance of the node i, to the nearest neighboring node. For the analysis performed in this paper different values were considered for the local support domain size (α_s), which vary from 4.0 to 10.0 with 0.5 increments, and the local quadrature/collocation domain size (α_q) which vary from 0.4 to 0.9999 with 0.05 increments.

Displacement and energy norms can be used for error estimation. These norms can be computed, respectively as

$$\|u\| = \left[\int_\Omega u^T u d\Omega\right]^{1/2} \tag{55}$$

$$\|\varepsilon\| = \left[\frac{1}{2}\int_\Omega \varepsilon^T D\varepsilon d\Omega\right]^{1/2} \tag{56}$$

The relative error for $\|u\|$ and $\|\varepsilon\|$ is given, respectively by

$$r_u = \frac{\|u_{num} - u_{exact}\|}{\|u_{exact}\|} \tag{57}$$

$$r_{\varepsilon} = \frac{\left\| \varepsilon_{num} - \varepsilon_{exact} \right\|}{\left\| \varepsilon_{exact} \right\|} \tag{58}$$

Cantilever Beam

A Cantilever beam showed in Fig. 6, is subjected to a parabolic traction at the free end. The principal properties are presented in Table 1 and the problem is solved for plane stress case.

Table 1. Properties of Cantilever Beam

Parameters	Values
Height, D	12 m
Length, L	48 m
Thickness, t	1 m
Load, P	1000 N
Modulus of Elasticity, E	30 MPa
Poisson`s Ratio, ν	0.3

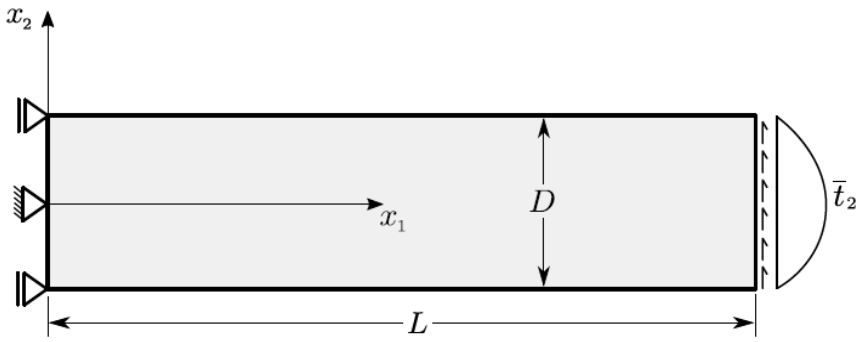

Figure 6. Cantilever beam

The parabolic traction and the moment of inertia is given by

$$\bar{t}_2(x_2) = -\frac{P}{2I}\left(\frac{D^2}{4} - x_2^2\right), \tag{59}$$

$$I = \frac{D^3}{12} \tag{60}$$

The exact solution of the problem is given by [19]. The equations for the exact displacement are:

$$u_1(x_1, x_2) = -\frac{Px_2}{6EI}\left[(6L - 3x_1) + (2+\nu)\left(x_2^2 - \frac{D^2}{4}\right)\right] \tag{61}$$

$$u_2(x_1, x_2) = \frac{P}{6EI}\left[3\nu x_2^2(L - x_1) + (4+5\nu)\frac{D^2 x_1}{4} + (3L - x_1)x_1^2\right] \tag{62}$$

The GSMF was used for solving this problem, five regular nodal distributions were considered with a discretization of 33 x 5 = 165 nodes, 65 x 9 = 585 nodes, 97 x 13 = 1261 nodes, 129 x 17 = 2193 nodes and 193 x 25 = 4825 nodes. The first discretization is showed in the Fig. 7.

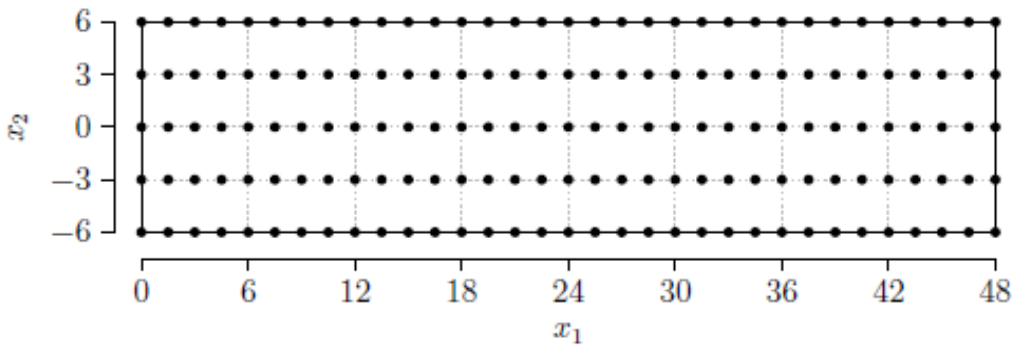

Figure 7. The regular nodal distribution of 33 x 5 = 165 nodes.

Influence of the local support domain size (α_s)

This parameter must be greater than 1.0, the reason is that for the small values, the algorithm of MLS approximation may be singular and the shape function cannot be constructed, because there is not enough nodes for the interpolation. The influence of α_s in the solution is obtained when the α_q is fixed.

Figure 8 shows the variation of relative error as a function of the size of the local support domain with 13 ratios which vary from 4.0 to 10.0 with 0.5 increments, and α_q = 0.5.

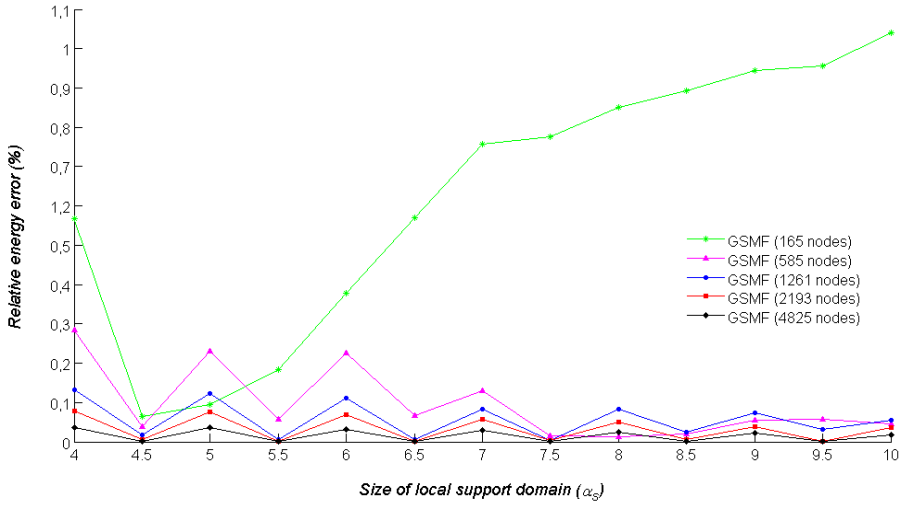

Figure 8. Analysis of the mesh - free discretization parameter α_s with α_q = 0.5 defined in equation (53), carried out with five regular discretization of the cantilever – beam, with 33 x 5 = 165, 65 x 9 = 585, 97 x 13 = 1261, 129 x 17 = 2193 and 193 x 25 = 4825 nodes.

Figure 8 shows that the value of 4.5 for the local support domain (α_s) presents low relative energy errors in the five regular discretization. The same graphic is obtained for the displacement.

Influence of the local quadrature/collocation domain size (α_q)

This parameter must be less than 1.0. The reason is to ensure that the local sub – domains of the internal nodes are entirely within the solution domain, without being intersected by the global boundary. The influence of α_q is obtained when the α_s is fixed.

Figure 9 shows the variation of relative energy error as a function of the size of the local quadrature/collocation domain with 13 ratios, which vary from 0.4 to 0.9999 with 0.05 increments, and fixed on $\alpha_q = 4.5$.

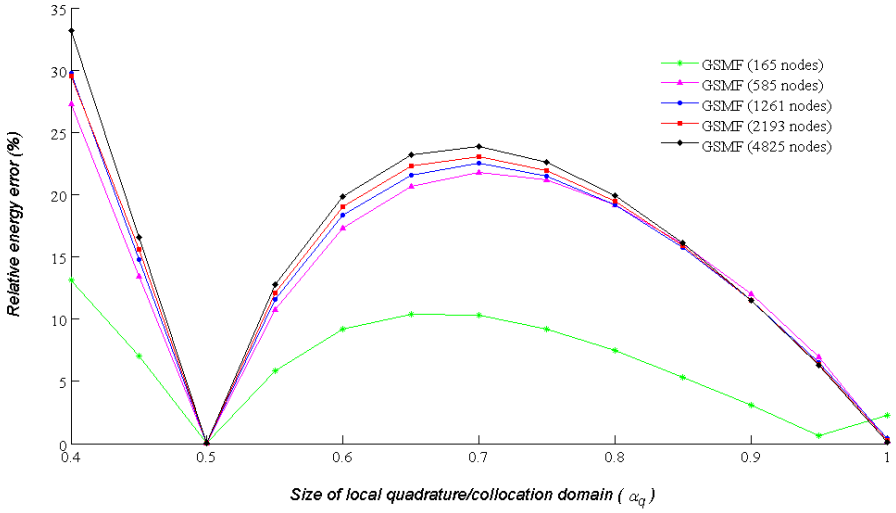

Figure 9. Analysis of the mesh - free discretization parameter α_q with $\alpha_s = 4.5$ defined in equation (54), carried out with five regular discretization of the cantilever – beam, with 33 x 5 = 165, 65 x 9 = 585, 97 x 13 = 1261, 129 x 17 = 2193 and 193 x 25 = 4825 nodes.

Figure 9 shows that the value of 0.5 for the local support domain (α_s) presents low relative energy errors in the five regular discretization. The same graphic is obtained for the displacement.

The Figure 10 and 11 presented the relative energy error suface for the nodal regular discretization with 97 x 13 = 1261 nodes, in one direction is presented the variation from 0.4 to 0.9999 for the size of local quadrature/collcation domain (α_q) and the other diretion the variation from 4 to 10 for the local support domain (α_s).

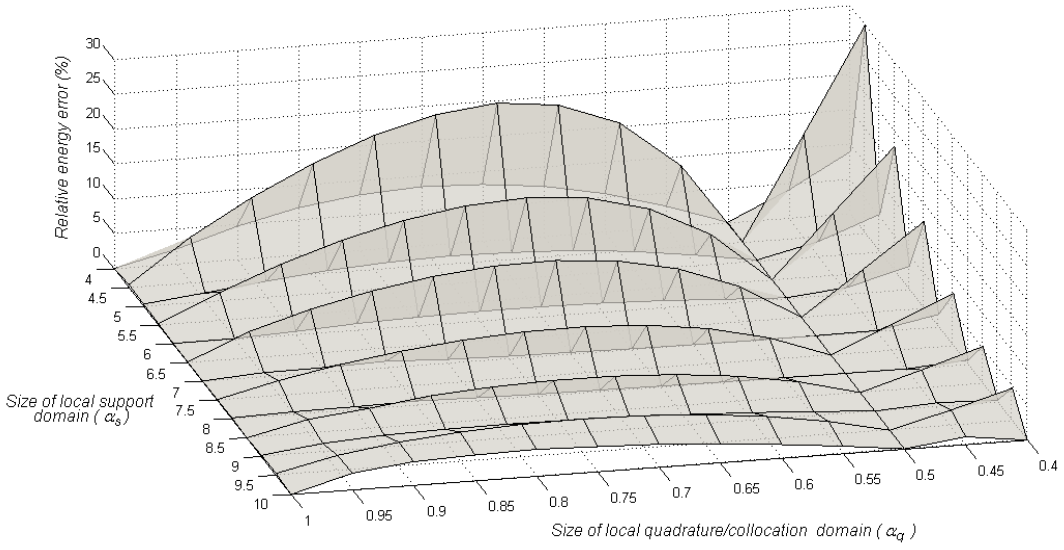

Figure 10. Analysis of the mesh - free discretization for parameters α_q and α_s, carried out by the regular discretization of the cantilever – beam, with 97 x 13 = 1261 nodes. Especial focus for the α_q parameter.

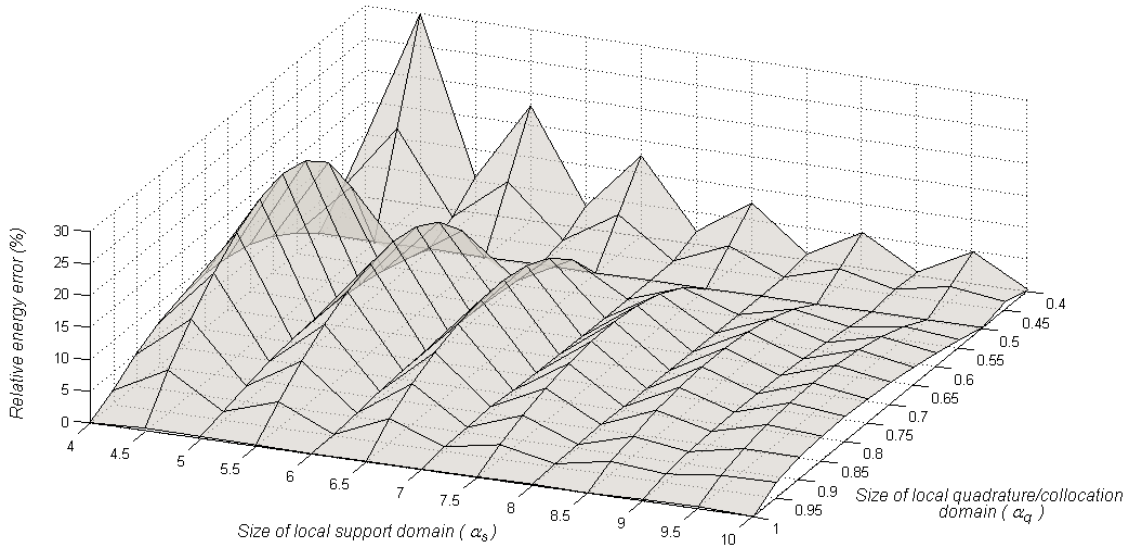

Figure 11. Analysis of the mesh - free discretization for parameters α_q and α_s, carried out by the regular discretization of the cantilever – beam, with 97 x 13 = 1261 nodes. Especial focus for the α_s parameter.

The Figure 11 and 12 shows a relative energy error surface in percentage for two different angles, the error for $\alpha_q = 0.5$ is always the lowest; as for the α_s there are different values, but the one that presents a greater efficiency is 4.5, because it results in a smaller CPU time consumption. Similar results were obtained for the relative displacement error.

Plate with a circular hole

Consider an infinite plate with a centered circular hole under unidirectional unit tension along the x1 direction, as represented in Fig. 12. Due to the symmetry of the problem about the horizontal and vertical axes, only a portion of the upper right quadrant of the plate is considered. The modeled section of the plate has dimensions b x b and the center circle has a radius a = 1, with b = 5a. The principal properties are presented in Table 2 and the problem is solved for plane stress case.

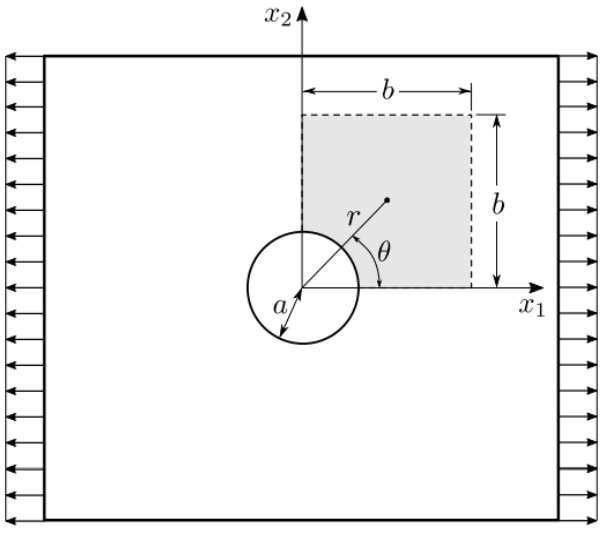

Figure 12. Plate with a hole.

Table 2. Properties of Plate with Circular Hole

Parameters	Values
Hole Radius, a	1 m
Height, D	5 m
Length, L	5 m
Thickness, t	1 m
Modulus of Elasticity, E	100000 Pa
Poisson`s Ratio, ν	0.25

The exact stress distribution in the plate is given by

$$\sigma_{11}(r,\theta) = 1 - \frac{a^2}{r^2}\left(\frac{3}{2}\cos 2\theta + \cos 4\theta\right) + \frac{3}{2}\frac{a^4}{r^4}\cos 4\theta \tag{63}$$

$$\sigma_{22}(r,\theta) = -\frac{a^2}{r^2}\left(\frac{1}{2}\cos 2\theta - \cos 4\theta\right) - \frac{3}{2}\frac{a^4}{r^4}\cos 4\theta \tag{64}$$

$$\sigma_{12}(r,\theta) = -\frac{a^2}{r^2}\left(\frac{1}{2}\cos 2\theta - \cos 4\theta\right) - \frac{3}{2}\frac{a^4}{r^4}\cos 4\theta \tag{65}$$

Where r and θ are the usual polar coordinates, centered at the center of the hole. A plane-stress state is considered which leads to the following displacements

$$u_1(r,\theta) = -\frac{\cos\theta}{2r^3E}\left[4a^4\cos^2\theta(1+\nu)(1-r^2) - 3a^4(1+\nu) + (ar)^2(1-3\nu) - 2r^4\right] \tag{66}$$

$$u_2(r,\theta) = -\frac{\sin\theta}{2r^3E}\left[4a^4\cos^2\theta(1+\nu)(1-r^2) - a^4(1+\nu) + (ar)^2(\nu-3) + 2r^4\nu\right] \tag{67}$$

The bottom and left edges of the plate are assumed as kinematic boundaries, with displacements specified on the bottom u_2 (x_1, x_2 = 0) and left edges (u_1 (x_1 = 0, x_1 = L, x_2) = 0). The rigid and top edges are assumed as static boundaries, loaded by tractions computed from the stresses of the exact solution (63, 64 e 65) as $t_j = \sigma_{ij,}$ in wich n_i represents the components of the unit outward normal to the edge of the plate.

The solve this problem, the plate was discretized by [17] with 9 nodes in the tangential direction and 11 nodes in the radial direction, see Fig. 13, with circular local supports. MLS approximation was considered, with the second order polynomial basis. GSMF was applied with 1 boundary collocation point per quadrant of the circular local domain.

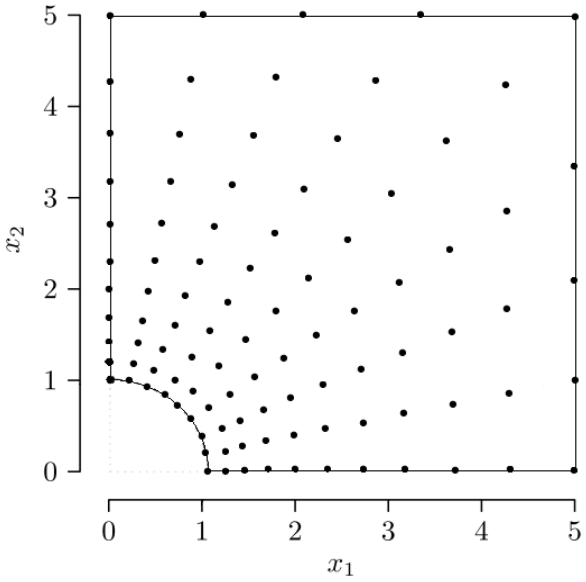

Figure 13. Nodal distribution for the infinite plate of 11x9 = 99 nodes.

The Figure 14 and 15 presented the relative energy error suface for the nodal regular discretization with 9 x 11 = 99 nodes, in one direction is presented the variation from 0.2 to 0.55 for the size of local quadrature/collocation domain (α_q) and the other diretion the variation from 3.5 to 6.0 for the local support domain (α_s).

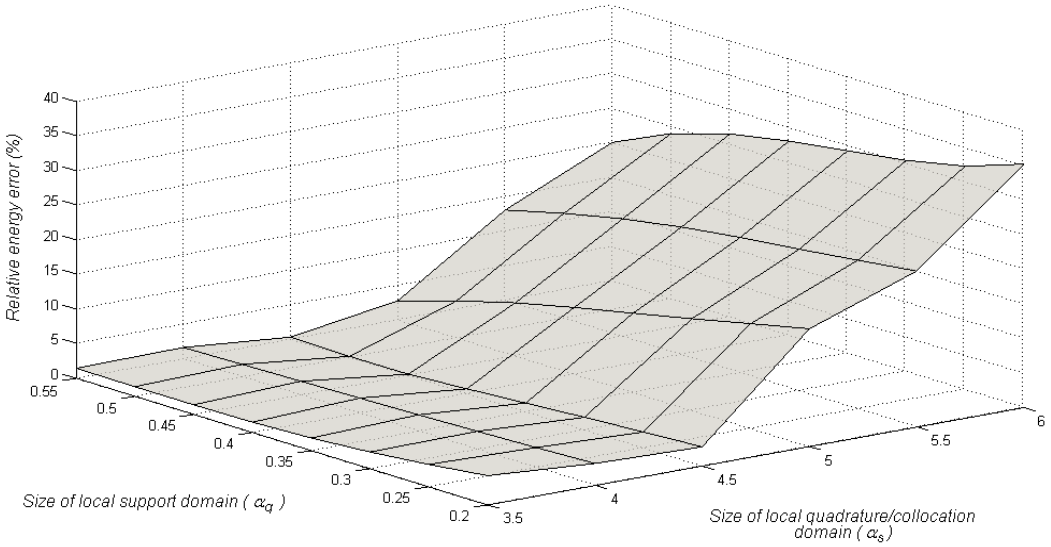

Figure 14. Analysis of the mesh - free discretization for parameters α_q and α_s, carried out by the regular discretization of the plate with a circular hole, with 9 x 11 = 99 nodes. Especial focus for the α_s parameter.

The Figure 14 and 15 shows the relative energy error surface in percentage for two different angles, the error for the α_s = 4.5 is always the least, for the α_s there are different values but the one that presents greater efficiency is 0.5 because present less CPU time consumption. Similar results were obtained for the relative displacement error.

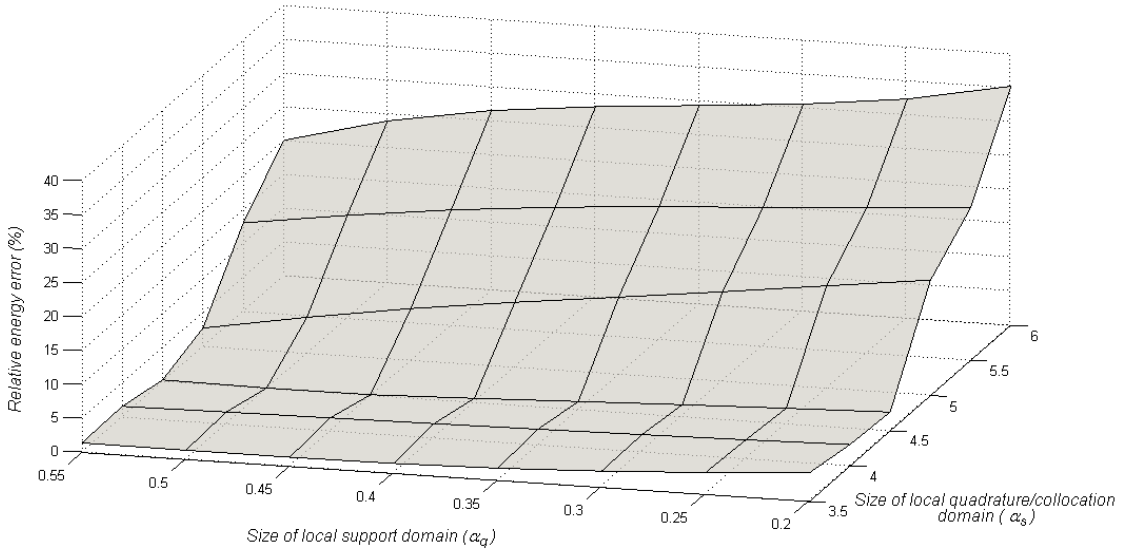

Figure 15. Analysis of the mesh - free discretization for parameters α_q and α_s, carried out by the regular discretization of the plate with a circular hole, with 9 **x** 11 = 99 nodes. Especial focus for the α_q parameter.

Conclusions

The size of local support domain (α_s) and local quadrature/collocation domain (α_q) affect the accuracy and performance of GSMF local method. For the different nodal discretization this parameters have a great influence in the relative energy and displacement error; but it is especially small for one particular values.

The special study realized for the cantilever beam discretized with 97 x 13 = 1261 nodes, presented greater variation in the relative energy error for different values of local support domain (α_s) and local quadrature/collocation domain (α_q). The parameter $\alpha_s = 0.5$ presented the lowest values independent of α_q value.

In this study were found certain values for the local support domain (α_s) and local quadrature/collocation domain (α_q) that generate less errors when the f method is applicate, these values are $\alpha_s = 4.5$ and $\alpha_q = 0$. It is necessary study others cases and other discretization especially for the plate with a circular hole.

Acknowledgments

The program PECC – *Pós-Graduação em Estruturas e Construção Civil*, Department of Civil and Environmental Engineering, Faculty of Technology, University of Brasília and CNPq – *Brazilian National Counsel of Technological and Scientific Development* for his PhD scholarship.

References

[1] Belytshko, T. Lu, Y. Y. and Gu, L. (1994) Element – free Galerkin methods, *International Journal for Numerical Methods in Engineering*, Vol. 20, 1081 – 1106.

[2] Atluri, S. N. and Shen, S. (2002) The Meshless Local Petrov – Galerkin (MLPG) Method: A simple and Less-costly Alternative to the Finite Element and Boundary Element Methods, *CMES: Computer Modeling in Engineering and Sciences*, Vol **3**(1), 11-51.

[3] Sladek, J. Sladek V. and Zhang, C. (2003) Application of Meshless Local Petrov – Galerking (MLPG) Method to Electrodynamic Problems in Continuously Non – Homogeneous Solids. *Computer Modeling in Engineering & Sciences*, Vol. **4**,637-648.

[4] Atluri, S. N. Han, Z. D. and Rajendram, A. M. (2004) A New Implementation of the Meshless Finite Volume Method Through the MLPG Mixed Approach, *CMES: Computer Modeling in Engineering and Sciences*, Vol **6**, 491-513.

[5] Alturi, S. N. (2004) The Meshless Method, (MLPG) for domain & BIE Discretizations, *Tech Science Press, Forsyth*.

[6] Atluri, S. N. Liu H. T. and Han Z. D. (2006) Meshless Local Petrov – Galerkin (MLPG) Mixed Collocation Method for Elasticity Problems, *CMES: Computer Modeling in Engineering and Sciences*, Vol **14**, 141-152.

[7] Liu, G. R. (2009) Meshfree methods moving beyond the finite element method. CRC Press, 2nd edition.

[8] Finalyson, B. A. (1972) The Method of Weighted Residuals and Vibrational Principles. Academic Press.

[9] Oliveira, T. and Portela, A. (2016) Weak – Form Collocation – a Local Meshless Method in Linear Elasticity, *Engineering Analysis with Boundary Elements*, 73: 144 – 160.

[10] Moussaoui, A. and Bouziane, T. (2013) Comparative Study of the Effect of the Parameters of Sizing Data on Results by the Meshless Methods (MLPG), *World Journal of Mechanics*, 3, 82-87.

[11] Erdayi, D. C. (2014) Meshless Local Petrov – Galerkin Method for Plane Elasticity Problems, Master Thesis, Middle East Technical University, Turkey, 2014.

[12] Fredholm, I. (1906) Solution d'un probléme fondamental de la théorie de l'éasticité, Arkiv for Matematik Astronomi och Fysk 2, 28(1):1-8.

[13] Fichera, G. (2006) Linear Elliptic Diferencial Systems and Eigenvalue Problems. Springer.

[14] Brebbia, C. A. and Tottenham, H. (1985) Variational Basis of Aproximate Models in Continuum Mechanics. Southampton and Springer Verlag.

[15] Gedalf, I. M. and Shilov, G. E. (1964) Generalized Functions, volume 1. Academic Press.

[16] Timoshenko, S. P. and Goodier, J. N. (1970). *Theory of Elasticity*, 3rd edn, McGraw-Hill, New York, USA.

[17] Alturi, S. N. and Zhu, T. L. (2000) The meshless local Petrov – Galerkin (MLPG) approach for solving problems in elasto – statics, *Computacional Mechanics*, 25:169-179.